Neutron Diffraction Study on the Structure of the Metallic Glass $Cu_{57}Zr_{43}$

P. Lamparter, S. Steeb, and E. Grallath
Max-Planck-Institut für Metallforschung, Institut für Werkstoffwissenschaften, Stuttgart

Z. Naturforsch. **38 a,** 1210–1222 (1983); received August 6, 1983

The structure of amorphous $Cu_{57}Zr_{43}$ has been investigated by neutron diffraction using the isotopic substitution method with the isotopes ^{63}Cu and ^{65}Cu besides natural Cu. From the scattering contribution of concentration fluctuations to the measured structure factors and from the atomic distances chemical ordering is concluded to exist in amorphous $Cu_{57}Zr_{43}$. The structural results are compared with previous experimental and theoretical investigations of Cu-Zr- and other binary metallic glasses formed by transition metals. Evidence is given that the topological as well as the chemical short range order is asymmetric in respect to both components in this type of metallic glasses.

Introduction

Metallic glasses from the Cu-Zr system, which can be produced since one decade [1, 2], are the most extensively studied ones belonging to the group of metal-metal alloys. The investigations involve the atomic structure by X-ray- [3–9] and neutron- [10, 11] diffraction as well as by EXAFS [12–15], dynamical properties by inelastic neutron diffraction [16, 17], inhomogeneities by small angle diffraction [18, 19], the glass forming ability [1, 20], the stability as well as the relaxation and crystallisation behaviour [21–34], magnetic [35–38], electronic [5, 38–49], mechanical [31, 50–52], thermodynamic [5, 30, 42, 53], and chemical [54–57] properties, superconductivity [58–60], NMR [61], positron annihilation [5, 62–65], Mössbauer spectroscopy [66], radiation damage [67], and technical applications [68–70]. Also a variety of theoretical studies on the structure [6, 71–74] and other properties [72, 73, 75, 76] can be found in the literature.

Despite the many publications dealing with Cu-Zr glasses one must state that their structure is not yet cleared up reliably. This is obvious from the contradictory structural results found in the literature up to now: Random mixing of both constituents follows from the values of coordination numbers by X-ray- [9] and neutron- [10, 11] diffraction as well as by EXAFS [12, 13]. On the other hand, also by X-ray diffraction [7, 8] and by EXAFS [14, 15] chemical short range order (CSRO) was found in Cu-Zr glasses. The case of statistical distribution of both kinds of atoms, however, is very unlikely because of the following reasons: Those scattering experiments performed up to now with metal-metal glasses which are, due to the scattering amplitudes of their constituents, sensitive to CSRO effects (Cu-Ti [77], Ni-Ti [78, 79], Ni-(Zr, Hf) [80]) all showed up the presence of CSRO. Furthermore, the electronic structure of amorphous Cu-Zr alloys [40, 41] reflects strong chemical interaction between the two kinds of atoms.

Generally there is growing evidence that the chemical interaction between the components of an alloy is an important condition for its glass forming ability.

Reprint requests to Prof. Dr. S. Steeb, Max-Planck-Institut für Metallforschung, Institut für Werkstoffwissenschaften, D-7000 Stuttgart 1.

Fundamentals

For convenience of discussion of the experimental results the essential equations are given in the following:

Faber Ziman Formalism

According to the Faber Ziman definition [81] the total structure factor is obtained from the coherently scattered intensity per atom $I^c(Q)$:

$$S^{FZ}(Q) = \frac{I^c(Q) - [\langle b^2\rangle - \langle b\rangle^2]}{\langle b\rangle^2}, \qquad (1)$$

where

Q $= 4\pi \sin\Theta/\lambda$,
2Θ = scattering angle,

0340-4811 / 83 / 1100-1210 $ 01.3 0/0. – Please order a reprint rather than making your own copy.

λ = wavelength of the radiation,
$\langle b \rangle = c_A b_A + c_B b_B$,
$\langle b^2 \rangle = c_A b_A^2 + c_B b_B^2$,
c_A, c_B = atomic concentrations of the components A and B,
b_A, b_B = coherent scattering lengths of A and B.

The total structure factor is a sum of the three weighted partial Faber Ziman structure factors $a_{ij}(Q)$:

$$S^{FZ}(Q) = \frac{c_A^2 b_A^2}{\langle b \rangle^2} a_{AA}(Q) + \frac{c_B^2 b_B^2}{\langle b \rangle^2} a_{BB}(Q) + \frac{2 c_A c_B b_A b_B}{\langle b \rangle^2} a_{AB}(Q). \quad (2)$$

The three partial pair correlation functions (ppcf) $G_{ij}(R)$ are defined as

$$G_{ij}(R) = 4\pi R \left[\frac{\varrho_{ij}(R)}{c_j} - \varrho_0 \right], \quad (3)$$

where

$\varrho_{ij}(R)$ = pair density distribution function of i–j pairs, i.e. number of j atoms per unit volume at distance R from an i atom,
ϱ_0 = mean atomic number density.

The $G_{ij}(R)$ are obtained from the partial structure factors by Fourier transformation

$$G_{ij}(R) = \frac{2}{\pi} \int_0^\infty Q [a_{ij}(Q) - 1] \sin(QR)\, dQ. \quad (4)$$

The interatomic distances are given by the positions of maxima of the $G_{ij}(R)$ functions.

The partial radial distribution functions $A_{ij}(R)$ can be calculated from the $G_{ij}(R)$:

$$A_{ij}(R) = c_j [4\pi R^2 \varrho_0 + R G_{ij}(R)]. \quad (5)$$

From $A_{ij}(R)$ the partial coordination number Z_{ij} can be evaluated:

$$Z_{ij} = \int_{R_l}^{R_u} A_{ij}(R)\, dR. \quad (6)$$

In the present work the minima besides the main peak of $A_{ij}(R)$ are taken as integration limits.

For the total functions $S^{FZ}(Q)$, $G(R)$, $A(R)$, and the total coordination number N also (4), (5), (6) are valid, whereby in (5) c_j has to be dropped.

Bhatia Thornton Formalism

Using the Bhatia Thornton formalism [82] the structure of a binary system is described in terms of correlations between density fluctuations and concentration fluctuations, the Fourier transforms of them in Q-space being the partial Bhatia Thornton structure factors $S_{NN}(Q)$, $S_{CC}(Q)$, and $S_{NC}(Q)$. Here another definition of the total structure factor is convenient:

$$S^{BT}(Q) = \frac{I^c(Q)}{\langle b^2 \rangle}, \quad (7)$$

which in terms of the partial structure factors is

$$S^{BT}(Q) = \frac{\langle b \rangle^2}{\langle b^2 \rangle} S_{NN}(Q) + \frac{c_A c_B (b_A - b_B)^2}{\langle b^2 \rangle} S_{CC}(Q) + \frac{2 \langle b \rangle (b_A - b_B)}{\langle b^2 \rangle} S_{NC}(Q), \quad (8)$$

where

$S_{NN}(Q)$ = partial structure factor of the correlations between number density fluctuations,
$S_{CC}(Q)$ = partial structure factor of the correlations between concentration fluctuations,
$S_{NC}(Q)$ = partial structure factor of the cross correlations between concentration fluctuations and density fluctuations.

The three density concentration correlation functions are obtained from the partial structure factors by Fourier transformation from Q-space to R-space:

$$G_{NN}(R) = \frac{2}{\pi} \int Q [S_{NN}(Q) - 1] \sin(QR)\, dQ,$$

$$G_{CC}(R) = \frac{2}{\pi} \int Q [S_{CC}(Q) - 1] \sin(QR)\, dQ,$$

$$G_{NC}(R) = \frac{2}{\pi} \int Q\, S_{NC}(Q) \sin(QR)\, dQ. \quad (9)$$

$G_{NN}(R)$ represents the topological short range ordering (TSRO), whereas $G_{CC}(R)$ represents the chemical short range ordering (CSRO). G_{NC} represents the size effect, which is caused by different atomic volumes of the components.

The description of the atomic structure of an amorphous binary in terms of the Bhatia Thornton partial functions has a clear meaning if the contribution of S_{NC} is zero or at least small, that means if the atomic diameters differ not too much. In this case the TSRO as well as the CSRO is symmetric in

respect to the two constituents and the alloy is designated as a substitutional one. The description of its structure only requires the two partial functions, S_{NN} and S_{CC}. On the other hand, the structure of an amorphous alloy whose components have very different atomic sizes may be better described in terms of the three Faber Ziman partial structure factors a_{AA}, a_{BB}, and a_{AB}.

Experiments and Data Reduction

Three amorphous $Cu_{57}Zr_{43}$ samples were produced by the melt-spinning technique in He atmosphere; one with copper with natural isotopic abundance (sample 2), one with the ^{63}Cu isotope (98.2% enriched, sample 1), and one with the ^{65}Cu isotope (96.7% enriched, sample 3). The ribbons were cut into small shreds and packed in vanadium tubes with 0.1 mm wall thickness, 42 mm height, and 11.5 mm outer diameter. The neutron diffraction experiments were performed with the D4 diffractometer at the Institute Laue Langevin, Grenoble [83]. Intensity profiles were recorded from $2\Theta = 1.3°$ up to 143° using neutrons with 0.69 Å wavelength. The counting statistic per measured point corresponded to 0.5 pct statistical error. The necessary corrections for the evaluation of the coherent intensity from the measured data were essentially the same as described earlier [84]. Smoothing of the measured curves was performed with a cubic spline fit procedure. For the macroscopic density the value 7.51 g/cm^3 was taken [85].

The absorption and scattering parameters of Cu and Zr used in the present work are listed in Table 1. As for the values of the scattering lengths b_i, which have to be known accurately in isotopic substitution experiments, the following comments should be given: The b_i-values of ^{nat}Cu, ^{63}Cu, and ^{65}Cu given in [86] turned out to be not consistent with the results of the present experiments. Therefore, a set of three consistent values was derived from the scattered intensities: The three specimens have been prepared in such a way that the mass of the Cu-Zr material exposed to the neutron beam was known. Therefore, the ratios $I_1^t(Q):I_2^t(Q):I_3^t(Q)$ of the total scattered intensities per atom could be evaluated. In the high-Q-region $I_i^t(Q)$ approaches to

$$I_i^t(\infty) = k\,[\langle b^2\rangle + (\langle\sigma^{inc}\rangle + \sigma^{ms})/4\pi]\,, \qquad (10)$$

where σ^{ms} is the multiple scattering contribution and k a normalization factor, which cancels out in the ratios. Using the values for σ^{inc} from Table 1 and assuming that the values $b(^{nat}Cu) = 0.768 \cdot 10^{-12}$ cm and $b(Zr) = 0.716 \cdot 10^{-12}$ cm are correct, a set of three coherent scattering lengths for the three Cu-materials was calculated, which was consistent with the ratios $I_1^t(\infty):I_2^t(\infty):I_3^t(\infty)$ and with (10). The b_i-values for the pure isotopes ^{63}Cu and ^{65}Cu (see Table 1) were then derived taking into account the isotopic enrichment of the Cu-materials used in the present work. It should be noted that the experimental value of σ^{inc} for ^{nat}Cu in Table 1 agrees with the corresponding one which can be calculated from σ^{inc} of ^{63}Cu and ^{65}Cu, whereby the isotopic incoherence has to be added. From this we conclude that the values for σ^{inc} in Table 1 which enter into the calculation of the values for b_i, according to (10), are correct. Finally, a consistency check can be made using (11):

$$b(^{nat}Cu) = 0.691\; b(^{63}Cu) + 0.309\; b(^{65}Cu)\,, \quad (11)$$

where the weighting factors are the natural isotopic abundances of ^{63}Cu and ^{65}Cu. This equation is fullfilled by the b_i-values given in Table 1, but not, for expamle, by the corresponding values reported in [86], which have been used by Kuodo et al. [10].

Table 1. Absorption- and scattering-parameters: σ^a = absorption cross section, σ^{inc} = incoherent scattering cross section, b = coherent scattering length. * See text.

Component	σ^a [barn] ($\lambda = 0.69$ Å)	σ^{inc} [barn]	b [10^{-12} cm]
Zr	0.064 [86]	0.11 [88]	0.716 [90]
^{nat}Cu	1.50 [87]	0.50 [88]	0.768 [88]
^{63}Cu (pure)	1.79 [87]	0.006 [89]	0.652 *
^{65}Cu (pure)	0.865 [87]	0.40 [89]	1.026 *
^{63}Cu (98.2% enr.)	1.77	0.013	0.659
^{65}Cu (96.7% enr.)	0.896	0.39	1.014

Results and Discussion

Structure Factors

From the coherently scattered intensities $I^c(Q)$ the total structure factors $S_n^{FZ}(Q)$ for the three alloys were calculated with (1) and plotted in Figure 1. To illustrate the statistical fluctuations of the measured data in the insert of Fig. 1, also part of

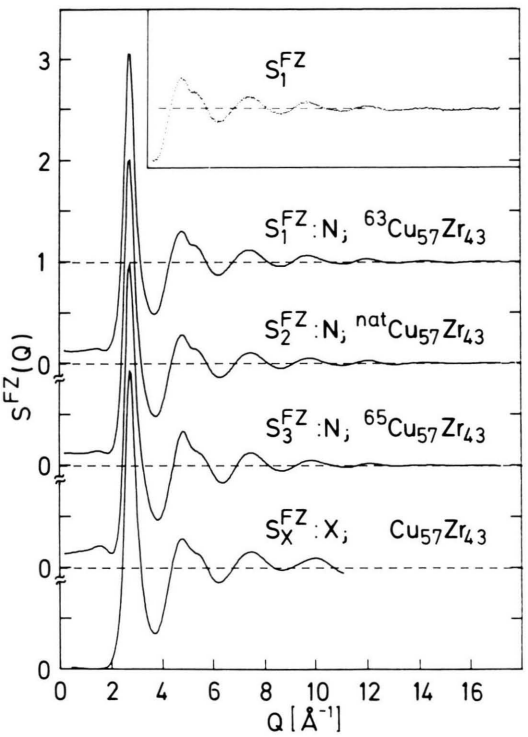

Fig. 1. Total structure factors $S^{FZ}(Q)$. N: Neutron diffraction, X: X-ray diffraction.

the unsmoothed measured $S_1^{FZ}(Q)$-curve is given. Furthermore, the total $S_X^{FZ}(Q)$ measured by X-ray diffraction with Mo-K_α-radiation is plotted.

Compared to the X-ray structure factor, the neutron structure factors show two remarkable features in the low-Q-region: Whereas S_X^{FZ} is zero at low Q's, S_1^{FZ}, S_2^{FZ}, and S_3^{FZ} extrapolate to 0.13. One may suppose that this behaviour is caused by a certain amount of hydrogen inserted during the preparation of the specimens which would in fact give rise to a constant background level due to the large incoherent neutron scattering cross section of hydrogen. A check of this problem was made by an additional neutron scattering experiment with a crystallized $^{nat}Cu_{57}Zr_{43}$ sample. After the background corrections – same σ^{ms} as for the amorphous sample but no subtraction of the Laue monotonic scattering term – the corresponding value for $S(Q)$ at low Q's was zero within the error limits. After crystallisation the sample contains at least the same hydrogen impurities as the amorphous samples. Therefore the high level of the neutron structure factors of the amorphous samples at low Q's is not caused by hydrogen but rather by the amorphous structure itself.

The second interesting feature of the neutron curves is the appearance of a so-called prepeak in front of the main maximum, which is not observed, however, with the X-ray curve. This prepeak, which is caused by concentration fluctuations, S_{CC}, clearly shows up the presence of a chemical short range order effect in amorphous $Cu_{57}Zr_{43}$. A rough estimation of the strength of the CSRO effect can be made by dividing the amplitude of the prepeak by the weighting factor of S_{CC} in (8). This shows that in spite of the small amplitudes of the prepeaks in Fig. 1 the CSRO nevertheless must be strong in amorphous Cu-Zr, because of the very small weighting factors (see (13a–c), below).

Corresponding to (2) the total $S_n^{FZ}(Q)$ obtained with specimen number n is expressed in terms of the partial structure factors $a_{ij}(Q)$:

$$S_1^{FZ}(Q) = 0.308\, a_{CuCu}(Q) + 0.198\, a_{ZrZr}(Q) + 0.494\, a_{CuZr}(Q), \quad (12a)$$

$$S_2^{FZ}(Q) = 0.346\, a_{CuCu}(Q) + 0.169\, a_{ZrZr}(Q) + 0.484\, a_{CuZr}(Q), \quad (12b)$$

$$S_3^{FZ}(Q) = 0.435\, a_{CuCu}(Q) + 0.116\, a_{ZrZr}(Q) + 0.449\, a_{CuZr}(Q), \quad (12c)$$

$$S_X^{FZ}(Q) = 0.240\, a_{CuCu}(Q) + 0.260\, a_{ZrZr}(Q) + 0.500\, a_{CuZr}(Q). \quad (12d)$$

Corresponding to (8) the total $S_n^{BT}(Q)$ are expressed in terms of the Bhatia Thornton partial structure factors:

$$S_1^{BT}(Q) = 0.998\, S_{NN}(Q) + 0.002\, S_{CC}(Q) - 0.164\, S_{NC}(Q), \quad (13a)$$

$$S_2^{BT}(Q) = 0.999\, S_{NN}(Q) + 0.001\, S_{CC}(Q) + 0.142\, S_{NC}(Q), \quad (13b)$$

$$S_3^{BT}(Q) = 0.973\, S_{NN}(Q) + 0.027\, S_{CC}(Q) + 0.656\, S_{NC}(Q), \quad (13c)$$

$$S_X^{BT}(Q) = 0.975\, S_{NN}(Q) + 0.025\, S_{CC}(Q) - 0.637\, S_{NC}(Q). \quad (13d)$$

The three neutron diffraction experiments, in principle, provide a set of three equations for the extraction of the three partials a_{ij}, (12a, b, c), and

of the three partials S_{NN}, S_{CC}, and S_{NC}, (13a, b, c). In practice, however, it turned out that it was not possible to extract reliable a_{ij}-functions. This can be understood from the fact that due to the badly conditioned system of the three equations (12a, b, c), whose normalized determinant has the very low value of $2 \cdot 10^{-3}$, even very small experimental uncertainties lead to drastic uncertainties in the resulting partial functions. It should be noted that even better counting statistics than that of the present work cannot overcome this problem, but that rather systematic errors in the correction procedures and in the tabulated scattering and absorption cross sections nowadays require a much better conditioned system of equations.

For the case of the Bhatia Thornton partial structure factors the coefficients in (13a, b, c) show that the evaluation of the partials S_{NN} and S_{NC} should be possible, whereas the contribution of S_{CC} is too small to allow its separation. This is readily seen from the value of the determinant which equals $7 \cdot 10^{-3}$ for the system of the three equations, but which becomes $3 \cdot 10^{-1}$ for (13a, b) for S_{NN} and S_{NC} alone when S_{CC} is neglected. Figure 2 shows the partials S_{NN} and S_{NC} resulting from (13a, b, c). The dotted part of the curves below $Q = 2$ Å^{-1} should indicate that in this range, where the prepeak occurs, the results are uncertain, because the main contribution of S_{CC} lies in this range and is thus there not necessarily small. The run of S_{NC} shows that the size effect in amorphous Cu-Zr, as expected from the difference of the atomic diameters, plays an important role in the structure. As this function frequently was theoretically calculated [79] or even neglected [77] in structural researches it is interesting to compare the experimental S_{NC}-function with the corresponding theoretical Ashcroft Langreth hard sphere function [91]. Figure 2 shows the result as dashed curve, whereby the atomic diameters were chosen as $d_{Cu} = 2.59$ Å and $d_{Zr} = 3.28$ Å, and the density as 7.51 g/cm^3. Comparison shows that the general features of both curves agree in the Q-range where the main peak of S_{NN} lies, but that the oscillations of the hard sphere S_{NC} are more pronounced by a factor two compared to those of the experimental curve.

The prepeak occuring in the S_n^{FZ} in Fig. 1 is most pronounced in the S_3 curve, which is in accordance with the fact that in this case the weighting factor of the S_{CC} function is larger than in S_1 and S_2 (see (13)). On the other hand, in the X-ray structure factor S_X^{BT} this weighting factor is as large as in S_3^{BT}, and nevertheless we observe even not a trace of a prepeak. This behaviour must be due to the contribution of the partial S_{NC}, which is as large in S_X^{BT} as in S_3^{BT} but opposite in sign, and we must conclude that in the X-ray case the oscillation of S_{CC} in front of the main peak is cancelled by that of S_{NC}.

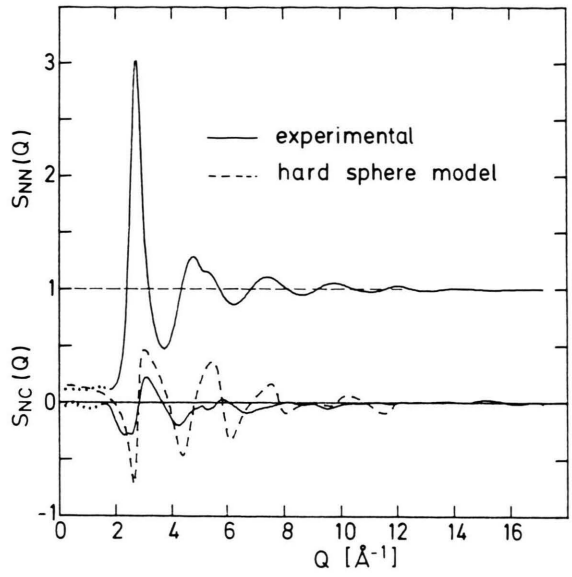

Fig. 2. a-$Cu_{37}Zr_{43}$: Bhatia Thornton partial structure factors $S_{NN}(Q)$ and $S_{NC}(Q)$.

Comparison of this observation with structural data for other amorphous metal-metal alloys found in the literature seems to be quite interesting and is shown in Table 2. All alloys have the common feature that the atomic diameter ratio is clearly below unity. We state that those alloys for which a CSRO effect is clearly demonstrated by neutron diffraction exhibit no prepeak in the X-ray diffraction case if the weighting factor of S_{NC} is large but negative, that means where the scattering power of the smaller constituent A is distinctly weaker than that of the larger constituent B. This observation again reflects the important role of the size effect in the structure of metal-metal glasses. From the foregoing one can show that the chemical ordering is asymmetric with respect to both constituents in that way that the oscillations of the S_{CC} function are mostly caused by a larger pseudoperiod of the ordering of the smaller component:

Table 2. d_i = atomic diameter; w_{ij} = weighting factors of the a_{ij} in Eqn. (2); w_{nc} = weighting factors of the partial structure factors in Eqn. (8); Q_p, Q_1 = position of the prepeak, main peak of $S(Q)$; I_p = amplitude of the prepeak measured from $S^{FZ}(Q \approx 0)$ as baseline. *$S(Q)$ defined according to Eqn. (7).

Sample A–B	$\frac{d_A}{d_B}$	X: X-ray N: Neutron	w_{ij} AA	BB	AB	w_{nc} NN	CC	NC	$\frac{b_A}{b_B}$	prepeak in $S(Q)$	$\frac{Q_p}{Q_1}$	I_p
$Cu_{57}Zr_{43}$	0.800	X	0.240	0.260	0.500	0.975	0.025	−0.637	0.725	No	–	–
this work		N (^{63}Cu)	0.308	0.198	0.494	0.998	0.002	−0.164	0.922	Yes	0.53	0.03
		N (^{nat}Cu)	0.346	0.169	0.484	0.999	0.001	0.142	1.074	Yes	0.55	0.03
		N (^{65}Cu)	0.435	0.116	0.449	0.975	0.027	0.656	1.418	Yes	0.58	0.08
$Ni_{60}Nb_{40}$	0.849	X	0.273	0.227	0.499	0.965	0.035	−0.756	0.683	No	–	–
[92]		N (^{nat}Ni)	0.470	0.099	0.431	0.967	0.033	0.735	1.493	Yes	0.62	0.10
		N (^{58}Ni)	0.566	0.061	0.372	0.907	0.093	1.190	2.087	Yes	0.62	0.18
$Ni_{35}Zr_{65}$	0.775	X	0.075	0.527	0.398	0.976	0.024	−0.654	0.700	No	–	–
[80]												
$Ni_{40}Ti_{60}$	0.844	X	0.211	0.293	0.497	0.986	0.014	0.485	1.273	Yes	0.62	0.11
[78, 79]		N	3.92	0.961	−3.883	0.088	0.912	1.155	−3.029	Yes	0.67	1.63*
$Co_{25}Ti_{75}$	0.850	X	0.084	0.504	0.412	0.991	0.009	0.426	1.227	Yes	0.59	0.06
[93]												
$Cu_{66}Ti_{34}$	0.871	X	0.530	0.074	0.396	0.985	0.015	0.517	1.318	Yes	0.59	0.06
X: [93], N: [77]		N	1.678	0.087	−0.766	0.357	0.643	0.643	−2.26	Yes	0.60	1.25*

We express S_{CC} and S_{NC} in terms of the a_{ij} for sake of simplification for the case of $c_A = c_B = 0.5$:

$$S_{CC} = 1 + (a_{AA} + a_{BB} - 2a_{AB})/4, \quad (14)$$

$$S_{NC} = (a_{AA} - a_{BB})/8. \quad (15)$$

We know that CSRO (pseudoperiod) leads to a positive peak of a_{AA} and a_{BB} and to a negative peak of a_{AB} in front of the main peak. These peaks sum up to the so-called S_{CC} prepeak, (14). If the CSRO is symmetric with respect to A and B, $a_{AA} = a_{BB}$ and $S_{NC} = 0$. But if the CSRO is asymmetric in such a way that $a_{AA} > a_{BB}$ in the range of the prepeak, then S_{NC} shows there, according to (15), also a peak, which may cancel that of S_{CC} if the factor w_{NC} of S_{NC} is large and negative. For the case of $a_{AA} < a_{BB}$, however, negative factor w_{NC} of S_{NC} would enhance the prepeak.

Finally we sum up these considerations by stating that the metal-metal amorphous alloys where one component is an early and one component is a late transition metal, do not belong to the substitutional type. It may be noted that this asymmetric structural behaviour is found to be much more rigorous in metallic glasses of the metal-metalloid type. In this type of glasses direct neighbourhood between the smaller metalloid atoms is avoided and thus the partial metalliod-metalloid structure factor shows a peak at lower Q-values than the main peak of the total X-ray structure factor [84]. It is therefore suggested that this asymmetric behaviour, more or less pronounced, is a common feature of all types of metallic glasses.

Correlation Functions

From the total structure factors $S^{FZ}(Q)$ the total correlation functions $G(R)$ were derived according to (4) and plotted in Figure 3. The total $G(R)$ are weighted sums of the $G_{ij}(R)$, where the weighting factors are the same as in (12a–d). Thus it is obvious that the calculation of the partial G_{ij} by solving a set of three equations analogous to (12a–c) fails as was already stated for the case of the partial structure factors a_{ij}. Figure 4a shows the main peak of the three neutron curves G_1, G_2, and G_3. They are slightly different, which can be understood by the weighting factors w_{ij} in (12): The rise of the level of the curves near $R = 2.6$ Å going from G_1 to G_2 and then to G_3 scales well with the rise of the weighting factor w_{CuCu} in (12a–c). This means that the main contribution of G_{CuCu} falls into this R-range. Simultaneously the shoulder at the right hand side near 3.2 Å decreases with decreasing w_{ZrZr}, which thus is identified as the contribution of G_{ZrZr}.

In order to determine the different atomic distances three difference curves Δ_1, Δ_2, and Δ_3 were

calculated choosing the factors of G_1 and G_3 in such a way that in each case one of the three G_{ij} cancels out. The three difference curves are plotted in Figure 4b.

$$\Delta_1 = G_3 - 0.910\, G_1 = 0.115\, G_{CuCu} - 0.064\, G_{ZrZr},$$

$$\Delta_2 = 1.411\, G_1 - G_3 = 0.248\, G_{CuZr} + 0.163\, G_{ZrZr},$$

$$\Delta_3 = 1.706\, G_3 - G_1 = 0.434\, G_{CuCu} + 0.273\, G_{CuZr}.$$

From Δ_1 the values $R_{CuCu} = 2.58$ Å (positive peak) and $R_{ZrZr} = 3.28$ Å (negative peak) and from Δ_2 the value $R_{CuZr} = 2.80$ Å were taken (see arrows). Δ_3 shows one peak at 2.67 Å which is formed by the two not resolved G_{CuCu} and G_{CuZr}. The atomic distance between unlike atoms (2.80 Å) is smaller than the mean value of the distances between like atoms (2.93 Å) by 5 ptc. This fact is explained by preferred chemical interaction between the two constituents in amorphous Cu-Zr.

Based on the known interatomic distances we tried to fit the first maximum of the total neutron-$G(R)$ curves by three partial $G_{ij}(R)$-curves: The starting curve was one constructed asymmetric function whose maximum position, height, and width was varied in order to produce three G_{ij} which reproduce the run of the total neutron curves. The results are shown in Fig. 5a, together with the experimental curves. The final values for R_{ij} and Z_{ij} thus obtained are listed in Table 3.

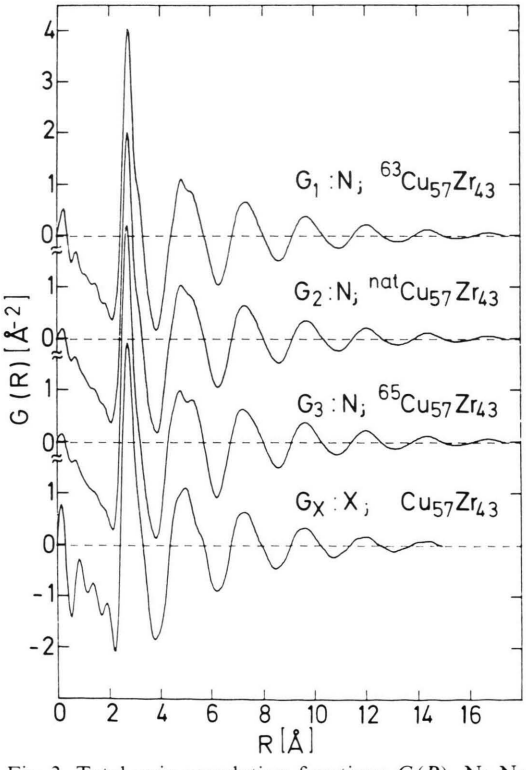

Fig. 3. Total pair correlation functions $G(R)$. N: Neutron diffraction, X: X-ray diffraction.

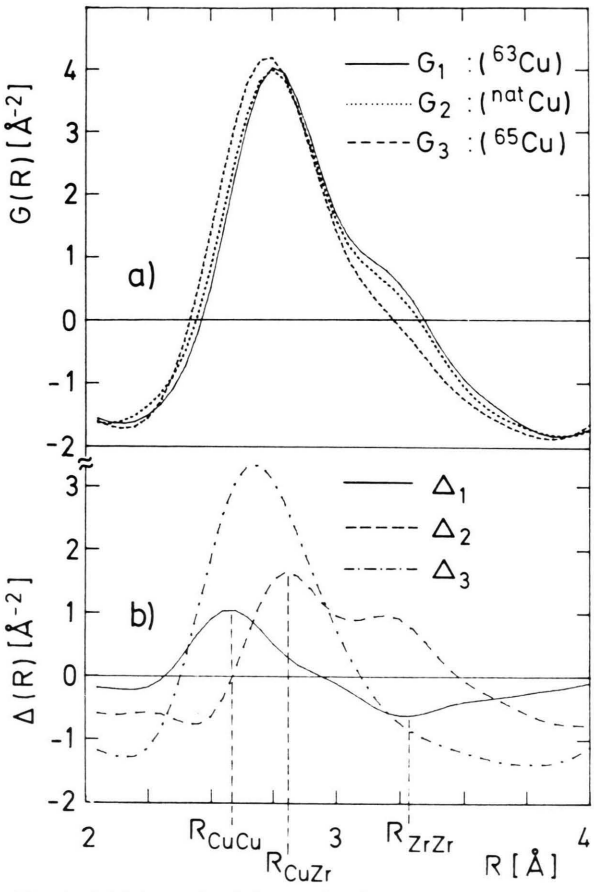

Fig. 4. a) Main peak of the total pair correlation functions from Fig. 3. b) Difference curves, see text.

It turned out that from the fit of the three measured total functions G_1, G_2, and G_3 in each case the same R_{ij} and widths resulted, but that different Z_{ij} had to be chosen to optimize the fit which led to the range given in Table 3 for their values. The fact that there is no unique set of three Z_{ij} which fits simultaneously the three total $G(R)$ again reflects the statement given above that straight-forward calculation of the $G_{ij}(R)$ from the totals was not possible. The resulting partials $G_{ij}(R)$ are plotted in Figure 5b.

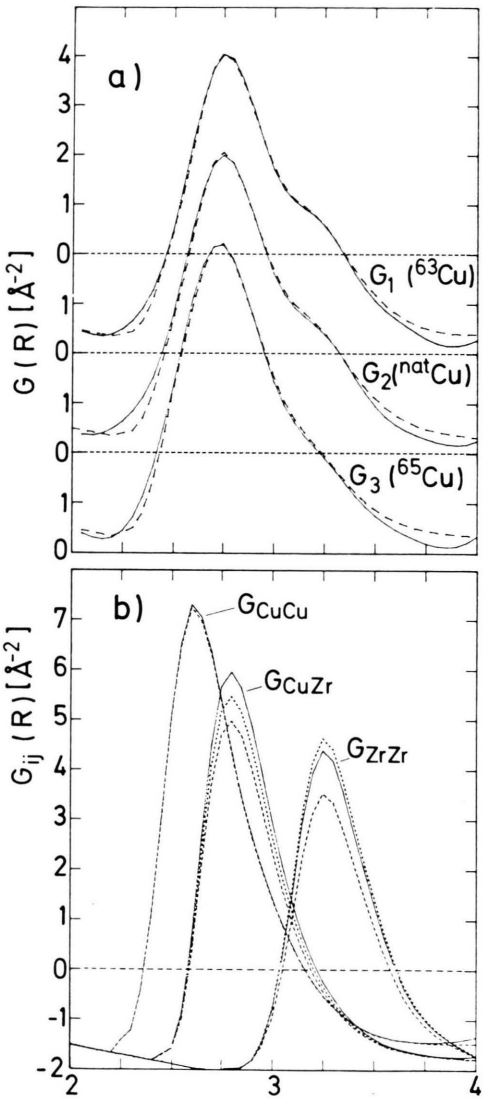

Fig. 5. a) Main peak of the total pair correlation functions. —— experimental from Fig. 3, – – – by fitting, see text. b) Partial pair correlation functions $G_{CuCu}(R)$, $G_{CuZr}(R)$, and G_{ZrZr}. —— by fitting of G_1, ··· of G_2, – – – of G_3.

From the partial Z_{ij} the Warren Cowley short range order parameter [94] α_i can be calculated referring either to a central Cu- or a central Zr-atom:

$$\alpha_i = 1 - \frac{Z_{ij}}{c_j(Z_{ij} + Z_{ii})}, \tag{16}$$

where i = Cu or Zr and j = Zr or Cu.

Table 3 shows that α_{Cu} as well as α_{Zr} comes out as nearly zero within the error bars. This result is in disagreement with the observed CSRO effect in Cu-Zr glasses, which means preference of unlike neighbours, i.e. negative values of α_i. Cargill and Spaepen [96] defined an alternative short range order parameter which accounts for the possibility that the ordering around both kinds of atoms may be different. It should be mentioned that with the partial coordination numbers of the present work also this parameter nearly becomes zero within the error bars.

Comparison with the Literature

A variety of experimental and theoretical studies on the structure of Cu-Zr glasses has been performed heretofore; the results of them shall be compared with the results of the present work in the following section. Hereby in Fig. 6a, b the first maximum of the curve G_1, where the shoulder at the right hand side, belonging to the Zr-Zr contribution is most distinctly observed, is chosen for the comparison. The atomic distances, the coordination numbers, and the resulting short range order parameters are summarized in Table 3. We note that the curves from the literature were taken graphically from plots and digitalized using a computer graphic input routine.

Experimental Data from Literature

Kudo et al. [10, 11] reported structure factors of $Cu_{57}Zr_{43}$ up to 11.4 Å^{-1} which were measured using the same isotopic substitution technique as in the present work. No hint on a prepeak was given by the authors. They derived partial G_{ij} functions as well as R_{ij}- and Z_{ij}-values (see Table 3). From the values of the Z_{ij} absence of CSRO was concluded in [11]. In Fig. 6a the main maximum of our experimental curve G_1 (solid line) is compared with a corresponding one which, according to (12a), was composed from the ppcf taken from [10] (line with small dots). Rather large differences are observed, especially at the right hand side, where the composed curve does not show a separate shoulder, maybe due to the relatively small R_{ZrZr} = 3.15 Å and the rather large widths of the G_{ij} in [10].

Chen et al. [8] estimated the ppcf for $Cu_{50}Zr_{50}$ by means of the anomalous X-ray scattering technique. Concerning this technique it should be noted that it yields a system of three equations for the

Table 3. Comparison between structural data of Cu-Zr glasses.

R_{CuCu}	R_{ZrZr}	R_{CuZr}	Z_{CuCu}	Z_{CuZr}	Z_{ZrCu}	Z_{ZrZr}	α_{Cu}	α_{Zr}	System	Reference
	[Å]			[atoms]						
2.59	3.28	2.77	8.1–8.3	4.7–5.4	6.2–7.1	4.8–5.7	0.11–0.15	0.01–0.05	$Cu_{57}Zr_{43}$	this work
2.65	3.15	2.80	5.4	5.0	6.7	5.9	−0.12	0.07	$Cu_{57}Zr_{43}$	[10, 11]
2.53	3.15	2.75	5.8	5.6	5.6	5.0	0.02	−0.06	$Cu_{50}Zr_{50}$	[8]
2.47	3.14	2.74	–	–	4.6	5.1	–	−0.03	$Cu_{46}Zr_{54}$	[13]
–	3.13	2.67	–	–	4.34	4.43	–	0.18	$Cu_{60}Zr_{40}$	[12]
2.52; 3.00	3.15	2.71; 3.05	3.75; 2	4.5; 2	7; 3	4	−0.33	−0.19	$Cu_{60}Zr_{40}$	[14, 15]
2.55	3.15	2.80	–	–	–	–	–	–	$Cu_{57}Zr_{43}$	[71]
2.63	3.24	2.80	4.9	5.4	5.4	7.7	−0.05	0.18	$Cu_{50}Zr_{50}$	[73]
2.43	3.04	2.75	–	–	–	–	–	–	$Cu_{57}Zr_{43}$	[74]
2.54	3.12	2.71	3.6	6.3	5.2	7.7	0.05	−0.22	$Cu_{33}Zr_{67}$	[72]

partial a_{ij} whose normalized determinant is worse by at least one order of magnitude than that of (12a–c). The values of the Z_{ij} (Table 3) were explained in [8] by a more or less random distribution of both kinds of atoms in Cu-Zr glasses, whereas preferred interaction of unlike atoms was concluded from the shape of the a_{ij}-curves. Figure 6a shows the total $G(R)$ of $Cu_{50}Zr_{50}$ (dashed line) composed from the partial G_{ij} from [8] with the appropriate weighting factors. The discrepancies between this curve and the experimental G_1 cannot be explained by the concentration difference alone.

Cu-Zr glasses have been also studied by EXAFS. Haensel et al. [13] fitted EXAFS data from $Cu_{46}Zr_{54}$ (Cu- and Zr-K-edge) by asymmetric correlation functions from which they got the figures in Table 3. They found correspondence of the coordination numbers with the composition of the alloy, which means random mixing, but different pair distribution characters, i.e. symmetric for Zr-Zr and asymmetric for Cu-Cu and Cu-Zr.

Wong et al. [12] reported EXAFS data from $Cu_{60}Zr_{40}$ (Zr-K-edge). The small value $R_{CuZr} = 2.67$ Å compared to the sum of the Goldschmidt radii of Cu and Zr is explained by chemical interaction. On the other hand they conclude random mixing of Cu and Zr from the scaling of coordination numbers with the composition of the glass.

Sadoc et al. [14, 15] proposed a two-subshell model for the quantitative description of their EXAFS data from $Cu_{60}Zr_{40}$ (Cu- and Zr-K-edge), where both for the Cu-Cu- and the Cu-Zr-distribution two coordination shells were taken (Table 3). As the coordination numbers of this model clearly yield negative values for α_{Cu} and α_{Zr} it is interesting

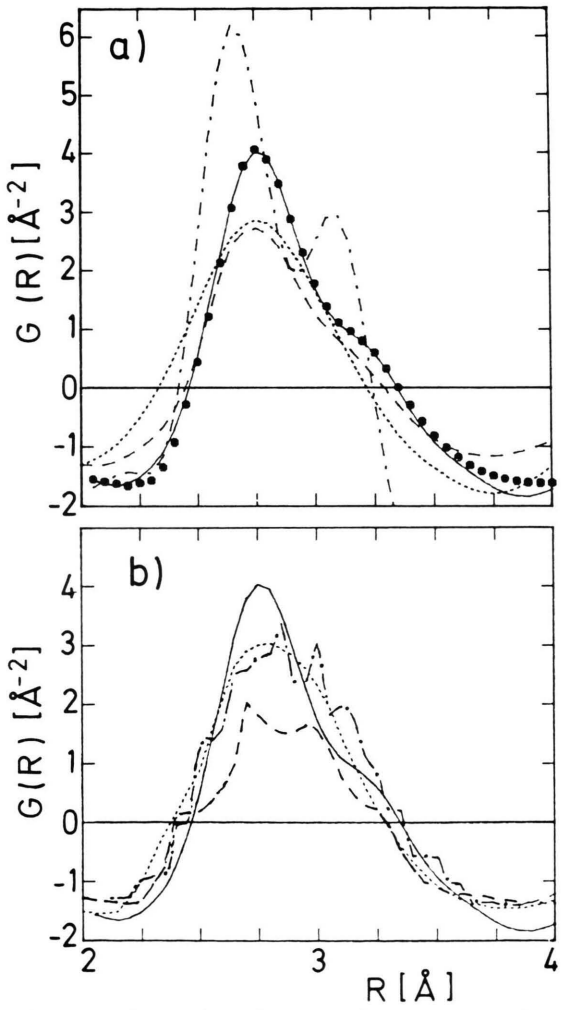

Fig. 6. a) Comparison between the present work and experimental data from literature. —— $G_1(R)$ from Figure 3. • Fit of $G_1(R)$ as in Figure 5a. Other curves see text. b) Comparison between the present work and theoretical data from literature. —— $G_1(R)$ from Figure 3. Other curves see text.

to check whether those Z_{ij} do fit the $G(R)$ curves obtained by neutron scattering. With the R_{ij}, Z_{ij}, and the widths σ_{ij} of the five distributions given in [15] a total $G(R)$ corresponding to $^{63}Cu_{60}Zr_{40}$ was simulated as sum of five Gaussian curves using the appropriate weighting factors. Mathematical details are described in previous papers [84, 95]. Figure 6a (dash dotted curve) shows the result, and one can see that the agreement is poor.

Resuming the experimental figures in Table 3 one can state that in each case the atomic distance of Cu-Zr pairs is smaller than the mean value of the Cu-Cu and Zr-Zr distances. This gives evidence for preferred interaction between unlike atoms in Cu-Zr glasses. From the partial coordination numbers, however, preferred coordination of unlike neighbours, which one would expect from the chemical interaction, cannot be concluded.

From (16) follows

$$\frac{\Delta\alpha_i}{\alpha_i} = \frac{1-\alpha_i}{\alpha_i} \frac{Z_{ii}}{Z_{ij}+Z_{ii}} \left[\frac{\Delta Z_{ij}}{Z_{ij}} + \frac{\Delta Z_{ii}}{Z_{ii}}\right], \qquad (17)$$

where Δ denotes an absolute error of the corresponding value.

If we assume the errors in the partial coordination numbers to be of the order of 10% and $Z_{ii} \approx Z_{ij}$, (17) yields as error in α_i 110%, 60%, and 43% for $\alpha_i = -0.1$, -0.2, and -0.3, respectively. This illustrates that small negative values of α_i lying in the range between -0.1 and -0.2 hardly can be evaluated from experimental partial coordination numbers.

Theoretical Data from Literature

Figure 6b shows besides the experimental correlation function $G_1(R)$ theoretical curves which were composed from partial pair correlation functions found in the literature up to now.

Kobayashi et al. [71] reported the ppcf of amorphous $Cu_{57}Zr_{43}$ obtained by a computer simulation study using modified Lennard-Jones 8-4 potentials between the atoms. Hereby the equilibrium Cu-Zr distance and the cohesive Cu-Zr energy were chosen as the average of the respective values for the Cu-Cu and Zr-Zr pairs. This implies that the model doesn't account for CSRO effects. Figure 6b (dashed line) shows that the peak for the resulting composed total $G(R)$ is lower than the experimental one.

Fujiwara et al. [73] calculated the ppcf by means of a relaxed dense random packing model for $Cu_{50}Zr_{50}$. The total $G(R)$ curve in Fig. 6b (dashed dotted line) is nearly as high as the experimental one, but the detailed features are not reproduced, which certainly is not due to the composition difference. The values of α_{Cu} and α_{Zr} for the model do not reflect a CSRO effect.

Beyer et al. [74] determined the partial pair correlation functions of $Cu_{57}Zr_{43}$ by molecular dynamic calculations based on Lennard-Jones 12-6 potentials. No special interaction between the Cu and the Zr atoms was introduced in the potential parameters, so that this model does not include CSRO effects. Accordingly the atomic distance between unlike atoms is the average of those between the like atoms. The $G(R)$ function in Fig. 6b (dotted line) according to the model exhibits a shoulder at its left hand side rather than at the right hand side, where the experimental one shows up the Zr-Zr contribution as a shoulder.

Harris et al. [72] used Lennard-Jones 12-6 potentials in a structure relaxation of a dense packing of hard spheres in order to simulate the structure of amorphous $Cu_{33}Zr_{67}$. They introduced CSRO by preferred interaction between unlike atoms. This is reflected by the value of R_{CuZr}, which is smaller than $(R_{CuCu} + R_{ZrZr})/2$, and also by the negative value of α_{Zr}, but not by the value of α_{Cu} (Table 3). Because of the rather large difference of the composition to that of the present work no composed $G(R)$ curve for this model is included in Figure 6b.

Summarizing the figures listed in Table 3, we state that the ten experimental and theoretical investigations, respectively, which are compared in this chapter, do not allow the extraction of the nature of the topological and chemical ordering within the first coordination shell of Cu-Zr glasses. Only R_{CuZr} shows the tendency to be smaller than the average of R_{CuCu} and R_{ZrZr}, which reflects the chemical interaction between Cu and Zr in amorphous Cu-Zr.

Conclusion

The isotopic substitution method has been applied in order to study the structure of amorphous $Cu_{57}Zr_{43}$. It turned out that the system of three equations was not conditioned well enough in view of the remaining experimental uncertainties, to

allow a straightforward calculation of the three partial correlation functions. Therefore, these three functions had to be estimated by a fitting procedure to the experimental total pair correlation functions. The Warren Cowley as well as the Cargill Spaepen short range order parameter were found to be in the range of zero.

On the other hand, the occurence of a prepeak in the neutron structure factors, which is caused by pronounced concentration fluctuations, as well as the evaluated atomic distances, showing preferred interaction between unlike atoms, give evidence for presence of a chemical short range order effect in the $Cu_{57}Zr_{43}$-glass. The review of experimental and theoretical data derived up to now for Cu-Zr glasses, including those of the present work, demonstrates that the kind of this chemical ordering is still unknown, although Cu-Zr glasses are the most comprehensively studied ones with two metallic components.

From the discussion of the prepeak occuring in the structure factors measured with neutrons, but not observed with X-rays, it is suggested that the size effect plays an important role in the amorphous structure. There is evidence that the topological as well as the chemical short range order is asymmetric with respect to the two components, the ordering of the smaller atoms rather exhibiting a larger pseudo-period than that of the larger atoms. Comparison with literature suggests that this behaviour is a common feature of metal-metal glasses. Further experimental investigations are needed, in which attention should be focussed on this question*.

Acknowledgement

Thanks are due to the Laue Langevin Institute, Grenoble, for allocation of beam time at the high flux reactor.

* *Note in addition:* During the completion of the present work we took note of a recent paper [97], where the authors pointed out that the contribution of the partial structure factor S_{NC} to the measured intensity of metal-metal glasses may play an important role in the region where the prepeak occurs.

[1] A. Revcolevschi and N. J. Grant, Met. Trans. **3,** 1545 (1972).
[2] R. Ray, B. C. Giessen, and N. J. Grant, Scripta Met. **2,** 357 (1968).
[3] Y. Waseda and T. Masumoto, Z. Phys. **B 21,** 235 (1975).
[4] Y. Waseda, T. Masumoto, and S. Tamaki, Liquid Metals, 1976, Inst. Phys. Conf. Ser. No. 30, 268 (1977).
[5] T. Mizoguchi, S. v. Molnar, G. S. Cargill III, T. Kudo, N. Shiotani, and H. Sakizawa, Amorphous Magnetism II, eds. R. A. Levy and R. Hasegawa, Plenum Press, New York 1977, p. 513.
[6] J. F. Sadoc and A. Liénard, Proc. 3rd Int. Conf. on Rapidly Quenched Metals, Brighton 1978, Vol. 2, p. 405.
[7] D. R. Chipman, L. D. Jennings, and B. C. Giessen, Bull. Amer. Phys. Soc. **23,** 467 (1978).
[8] H. S. Chen and Y. Waseda, Phys. Stat. Sol. (a) **51,** 593 (1979).
[9] L. Dargel-Sulir, M. Pyka, and A. Kozlowski, Acta Physica Polonica **A 62,** 81 (1982).
[10] T. Kudo, T. Mizoguchi, N. Watanabe, N. Niimura, M. Misawa, and K. Suzuki, J. Phys. Soc. Japan Lett. **45,** 1773 (1978).
[11] T. Mizoguchi, T. Kudo, T. Irisawa, N. Watanabe, N. Niimura, M. Misawa, and K. Suzuki, Proc. 3rd Int. Conf. on Rapidly Quenched Metals, Brighton 1978, Vol. 2, p. 384.
[12] J. Wong, F. W. Lytle, H. H. Liebermann, and L. E. Tanner, Proc. Conf. on Metallic Glasses, Science and Technology, Budapest 1980, Vol. 1, p. 383.
[13] R. Haensel, P. Rabe, G. Tolkiehn, and A. Werner, Proc. NATO Adv. Study Institute, Liquid and Amorphous Metals, eds. E. Lüscher and H. Coufal, 1980, p. 459.
[14] A. M. Flank, P. Lagarde, D. Raoux, J. Rivory, and A. Sadoc, Proc. 4th Int. Conf. on Rapidly Quenched Metals, Sendai 1981, p. 393.
[15] A. Sadoc, D. Raoux, P. Lagarde, and A. Fontaine, J. Non-Cryst. Sol. **50,** 331 (1982).
[16] J. B. Suck, H. Rudin, H.-J. Güntherodt, H. Beck, J. Daubert, and W. Gläser, J. Phys. C: Sol. State Phys. **13,** L 167 (1980), and Proc. Nato Adv. Study Institute, Liquid and Amorphous Metals, eds. E. Lüscher and H. Coufal, 1980, p. 649.
[17] T. M. Holden, J. S. Dugdale, G. C. Hallam, and D. Pavuna, J. Phys. F: Metal Phys. **11,** 1737 (1981).
[18] A. M. Flank and A. Naudon, J. de Physique C 8, **41,** 123 (1980).
[19] A. Naudon and A. M. Flank, Proc. 4th Int. Conf. on Rapidly Quenched Metals, Sendai 1981, p. 425.
[20] Y. Nishi, T. Mohoroshi, M. Kawakami, K. Suzuki, and T. Masumoto, ibid., p. 111.
[21] R. V. Raman, Ph.D. Thesis, Northeastern University, Boston, Massachusetts, 1974.
[22] J. M. Vitek, J. B. Vander Sande, and N. J. Grant, Acta Met. **23,** 165 (1975).
[23] B. C. Giessen, J. Hong, L. Kabacoff, D. E. Polk, R. V. Raman, and R. St. Amand, Proc. 3rd Int. Conf. on Rapidly Quenched Metals, Brighton 1978, Vol. 1, p. 249.
[24] P. G. Zieliński, J. Ostatek, M. Kijek, and H. Matya, ibid., p. 337.
[25] O. Hunderi and K. Lønvik, ibid., p. 375.
[26] N. H. Pratten and M. G. Scott, ibid., p. 387.
[27] N. H. Pratten and M. G. Scott, Scripta Met. **12,** 137 (1978).
[28] R. L. Freed and J. B. Vander Sande, J. Non-Cryst. Sol. **27,** 9 (1978).

[29] A. J. Kerns, D. E. Polk, R. Ray, and B. C. Giessen, Mater. Sci. Eng. **38,** 49 (1979).
[30] Y. Calvayrac, M. Harmelin, A. Quivy, J.-P. Chevalier, and J. Bigot, J. de Physique C 8, **41,** 114 (1980).
[31] A. Kursomovik and M. G. Scott, Proc. Conf. on Metallic Glasses, Science and Technology, Budapest 1980, Vol. 2, p. 275.
[32] J. W. Drijver, A. L. Mulder, and S. Radelaar, Proc. 4th Int. Conf. on Rapidly Quenched Metals, Sendai 1981, p. 535.
[33] R. C. Budhani, T. C. Goel, and K. L. Chopra, ibid., p. 615.
[34] W. Jingtang, W. Shueli, D. Bingzhe, and L. Shuling, ibid., p. 731.
[35] T. Mizoguchi and T. Kudo, AIP Conf. Proc. **29,** 167 (1976).
[36] F. R. Szofran et al., Phys. Rev. B (1976).
[37] E. M. Savitskii, Yu. E. Efimov, G. G. Mukhin, T. M. Frolova, and S. A. Turanov, Proc. Conf. on Metallic Glasses, Science and Technology, Budapest 1980, Vol. 1, p. 241.
[38] E. Babic, R. Ristic, M. Miljak, and M. G. Scott, Proc. 4th Int. Conf. on Rapidly Quenched Metals, Sendai 1981, p. 1079.
[39] A. Amamou and G. Krill, Solid State Comm. **28,** 957 (1978), and Solid State Comm. **33,** 1029 (1980).
[40] P. Oelhafen, E. Hauser, H.-J. Güntherodt, and K. H. Bennemann, Phys. Rev. Lett. **43,** 1134 (1979).
[41] P. Oelhafen, Proc. NATO Adv. Study Institute, Liquid and Amorphous Metals, eds. E. Lüscher and H. Coufal, 1980, p. 447.
[42] P. Garoche, Y. Calvayrac, and J. J. Keissié, J. de Physique C 8, **41,** 766 (1980).
[43] H.-J. Güntherodt, P. Oelhafen, R. Lapka, H. U. Künzi, G. Indelkofer, J. Krieg, T. Laubscher, H. Rudin, U. Gubler, F. Rösel, K. P. Ackermann, B. Delley, M. Fischer, F. Greuter, E. Hauser, M. Liard, M. Müller, J. Kübler, K. H. Bennemann, and C. F. Hague, ibid., p. 381.
[44] J. P. Carini, S. Basak, and S. R. Nagel, ibid., p. 463.
[45] K. Pękata and R. Trykozko, Proc. Conf. on Metallic Glasses, Science and Technology, Budapest 1980, Vol. 1, p. 459.
[46] G. Fritsch, J. Willer, A. Wildermuth, and E. Lüscher, in: Physics of Solids under High Pressure, eds. J. S. Schilling and R. N. Shelton, North-Holland, Amsterdam 1981, p. 239.
[47] J. Willer, G. Fritsch, and E. Lüscher, . Non-Cryst. Sol. **46,** 321 (1981).
[48] J. S. Dugdale, B. L. Gallagher, D. Greig, G. J. Morgan, and D. Pavuna, Proc. 4th Int. Conf. on Rapidly Quenched Metals, Sendai 1981, p. 1283.
[49] J. Rivory and J. M. Frigerio, ibid., p. 1287.
[50] J. Megusar, J. B. Vander Sande, and N. J. Grant, Proc. 2nd Int. Conf. on Rapidly Quenched Metals, Cambridge USA 1975, p. 401.
[51] H. U. Künzi, Proc. NATO Adv. Study Institute, Liquid and Amorphous Metals, eds. E. Lüscher and H. Coufal, 1980, p. 435.
[52] E. Girt, P. Tomić, T. Mihać, and A. Kuršomović, Proc. 4th Int. Conf. on Rapidly Quenched Metals, Sendai 1981, p. 487.
[53] P. Garoche, Thèse d'Etat, Orsay, 1981.
[54] M. Naka, K. Hashimoto, and T. Masumoto, J. Non-Cryst. Sol. **30,** 29 (1978).
[55] D. E. Polk, C. E. Dube, and B. C. Giessen, Proc. 3rd Int. Conf. on Rapidly Quenched Metals, Brighton 1978, Vol. 1, p. 220.
[56] F. H. M. Spit, J. W. Drijver, W. C. Turkenburg, and S. Radelaar, J. de Physique C 8, **41,** 890 (1980).
[57] J. Bigot, Y. Calvayrac, M. Harmelin, J.-P. Chevalier, and A. Quivy, Proc. 4th Int. Conf. on Rapidly Quenched Metals, Sendai 1981, p. 1463.
[58] H. v. Löhneysen, M. Platte, W. Sander, H. J. Schink, G. v. Minnigerode, and K. Samwer, J. de Physique C 8, **41,** 745 (1980).
[59] J. Kästner, H. v. Löhneysen, M. Platte, and K. Samwer, Proc. Conf. on Metallic Glasses, Science and Technology, Budapest 1980, Vol. 1, p. 439.
[60] J. D. Meyer, J. de Physique C 8, **41,** 762 (1980).
[61] J. Abart, W. Socher, and J. Voitländer, Z. Naturforsch. **37a,** 1030 (1982).
[62] S. Tanigawa, K. Hinode, R. Nagai, M. Doyama, and N. Shitani, Phys. Stat. Sol. (a) **51,** 249 (1979).
[63] W. Triftshäuser and G. Kögel, Proc. Conf. on Metallic Glasses, Science and Technology, Budapest 1980, Vol. 1, p. 347.
[64] E. Cartier, F. Heinrich, and H.-J. Güntherodt, Phys. Letters **81 A,** 393 (1981).
[65] K. Shima and S. Tanigawa, Proc. 4th Int. Conf. on Rapidly Quenched Metals, Sendai 1981, p. 543.
[66] B. C. Giessen, A. E. Attard, and R. Ray, Proc. 2nd Int. Conf. on Rapidly Quenched Metals, Cambridge USA 1975, p. 351.
[67] J. Hillairet, E. Balanzat, J. Bigot, and H. U. Künzi, J. de Physique C 8, **41,** 854 (1980).
[68] H. J. Schmidt, E. Henrich, T. Fritsch, F. Gompf, B. Renker, and E. Mohs, J. de Physique C 8, **41,** 886 (1980).
[69] S. A. Miller and R. J. Miller, Scripta Met. **13,** 673 (1979).
[70] S. A. Miller and R. J. Murphy, Proc. 4th Int. Conf. on Rapidly Quenched Metals, Sendai 1981, p. 137.
[71] S. Kobayashi, K. Maeda, and S. Takeuchi, J. Phys. Soc. Japan **48,** 1147 (1980).
[72] R. Harris and L. J. Lewis, Phys. Rev. **B 25,** 4997 (1982).
[73] T. Fujiwara, H. S. Chen, and Y. Waseda, J. Phys. F: Metal Phys. **13,** 97 (1983).
[74] O. Beyer and C. Hoheisel, Z. Naturforsch. **38a,** 859 (1983).
[75] S. Kobayashi, K. Maeda, and S. Takeuchi, Acta Met. **28,** 1641 (1980).
[76] S. Kobayashi and S. Takeuchi, Proc. 4th Int. Conf. on Rapidly Quenched Metals, Sendai 1981, p. 505.
[77] M. Sakata, N. Cowlam, and H. A. Davies, Proc. 4th Int. Conf. on Rapidly Quenched Metals, Sendai 1981, p. 327.
[78] H. Ruppersberg, D. Lee, and C. N. J. Wagner, J. Phys. F: Metal Phys. **10,** 1645 (1980).
[79] C. N. J. Wagner, D. Lee, L. Keller, L. E. Tanner, and H. Ruppersberg, Proc. 4th Int. Conf. on Rapidly Quenched Metals, Sendai 1981, p. 331.
[80] C. N. J. Wagner and D. Lee, J. de Physique C 8, **41,** 242 (1980).
[81] T. E. Faber and J. M. Ziman, Phil. Mag. **11,** 153 (1965).
[82] A. Bhatia and D. E. Thornton, Phys. Rev. **B 2,** 3004 (1970).
[83] Neutron Beam Facilities at the HFR available for Users, ILL, Grenoble 1981.
[84] P. Lamparter, W. Sperl, and S. Steeb, Z. Naturforsch. **37a,** 1223 (1982).
[85] H.-R. Hilzinger, Vakuumschmelze GmbH, Hanau, Germany, priv. comm.
[86] G. E. Bacon, Neutron Diffraction, 3rd ed., Clarendon Press, Oxford 1975.

[87] W. Knoll and S. Steeb, Z. Naturforsch. **33a,** 472 (1978).
[88] L. Koester, in Neutron Physics, Springer Tracts in Modern Physics **80,** 1 (1977).
[89] Calculated from the spin dependent scattering lengths taken from: H. Glättli, G. L. Bachella, M. Fourmond, A. Malinovski, P. Mériel, M. Pinot, P. Roubeau, and A. Abragam, J. de Physique **40,** 629 (1979).
[90] L. Koester, Reaktorstation, Garching, Germany, priv. comm.
[91] N. W. Ashcroft and D. C. Langreth, Phys. Rev. **155,** 685 (1967).
[92] F. Forgács, F. Hajdu, E. Sváb, and J. Takács, Proc. Conf. on Metallic Glasses, Science and Technology, Budapest 1980, Vol. 1, p. 283.
[93] A. Müller, P. Lamparter, and S. Steeb, to be published.
[94] J. M. Cowley, J. Appl. Phys. **21,** 24 (1950).
[95] E. Nassif, P. Lamparter, W. Sperl, and S. Steeb, Z. Naturforsch. **38a,** 142 (1982).
[96] G. S. Cargill III and F. Spaepen, J. Non-Cryst. Sol. **43,** 91 (1981).
[97] H. Ruppersberg and C. N. J. Wagner, J. Non-Cryst. Sol. **55,** 165 (1983).